Pre-normative REsearch for Safe use of Liquid Hydrogen (PRESLHY)

Project Deliverable

Experimental Investigation of Ignition of Cryogenic Hydrogen

Deliverable Number:	D26 (D4.3)
Work Package:	4
Version:	1.0
Author(s), Institution(s):	J Welch (HSE), P Hooker (HSE)
Submission Date:	07/2021
Due Date:	06/2021
Report Classification:	Public

This project has received funding from the Fuel Cells and Hydrogen 2 Joint Undertaking under the European Union's Horizon 2020 research and innovation programme under grant agreement No 779613.

History		
Nr.	Date	Changes/Author
0.1 – Draft HSE Report EA/21/10	20/05/2021	Original version
0.2 - Draft	09/06/2021	Technical Changes
0.3 - Draft	25/06/2021	Editorial Changes
1.0		First issue

Approvals			
Version	Name	Organisation	Date
1.0	E de Lewandowicz	HSE	28/07/2021

Acknowledgements

This project has received funding from the Fuel Cells and Hydrogen 2 Joint Undertaking under the European Union's Horizon 2020 research and innovation programme under grant agreement No 779613. The HSE work programme acknowledges funding from its sponsors Shell, Lloyd's and Equinor; and for instrumentation provided by NREL and Dräger.

Disclaimer

The data management in the PRESLHY project follows the principle of data management, which shall make data Findable, Accessible, Interoperable and Re-usable (FAIR). The plan for FAIR data management as described in this document is based on the corresponding template for open research data management plan (DMP) of the European Research Council (ERC).

Despite the care that was taken while preparing this document the following disclaimer applies: The information in this document is provided as is and no guarantee or warranty is given that the information is fit for any particular purpose. The user thereof employs the information at their sole risk and liability.

The document reflects only the views of the authors. The FCH JU and the European Union are not liable for any use that may be made of the information contained therein.

This report, and the work it describes, were undertaken by the Health and Safety Executive Science Division (HSE-SD) as part of the PRESLHY project. Its contents, including any opinions and/or conclusions expressed, or recommendations made, do not supersede current HSE policy or guidance.

Key words

FAIR data management, liquid hydrogen, accidental behaviour, release, ignition, combustion, electrostatic, pre-normative research, experimental data, accessibility, re-use, long-term data storage, research data repository.

Publishable Short Summary

Work package 4 of the PRESLHY project focuses on the ignition phenomena of cryogenic hydrogen.

This report summarises the results of experiments and analyses carried out as part of the PRESLHY work package 4 deliverables.

The report is divided into three parts, followed by a conclusions section that summarises the main conclusions from work package 4.

Part 1: Flammable properties of hydrogen, and hydrogen in air mixtures, at temperatures ranging from ambient down to cryogenic

In this section the influence of temperature on the flammable limits and minimum ignition energy of hydrogen, and hydrogen in air mixtures, are considered. The influence of the concentration of hydrogen in air mixtures, at ambient and low temperatures on the minimum ignition energy and the hot surface ignition temperature are also assessed.

Part 2: Environmental considerations and interactions regarding cryogenic hydrogen

In this section the interaction of cryogenic liquids with their environment upon release are considered. The influence of the substate onto which the cryogenic hydrogen is released, and the formation and composition of condensed air deposits on the substrate surface are assessed. The interaction between cryogenic hydrogen pools and water sprays are also considered.

Part 3: Charge generation and accumulation in cryogenic hydrogen

In this section the generation and accumulation of electrostatic charges in pools of hydrogen and multi-phase jets are considered. The influence of the initial temperature and pressure of the hydrogen on electrostatic charge build up during release scenarios are assessed. The influence of the size of the release orifice, in this case the nozzle diameter, are also considered.

Table of Contents

1. Introduction

The PRESLHY project experimental programme has been designed to provide insight and data on knowledge gaps within high-risk scenarios regarding the storage and transport of cryogenic liquid hydrogen. Previous theoretical work carried out as part of the PRESLHY project identified areas for which there was a lack of detailed experimental data and these areas were then the focus of the experimental work: previous studies found in the literature were discussed in detail in PRESLHY deliverable D4.1 (Lyons, et al., 2020).

The outstanding experimental work identified by Lyons et al included:

- Determination of the relationship between minimum ignition energy (MIE) and hot surface ignition on the initial mixture temperature.
- Assessment of the process of electrostatic charging and how this is affected by solids formation and breakup.
- How the generation of a charge in a flowing stream relates to the probability of an ignition event; and
- A recommendation for generation of empirical data to further investigate the behaviour and composition of pool and solid formations that form following a release of liquid hydrogen.

The resulting experimental programme designed for PRESLHY deliverable D4 covered a range of technical areas and a series of reports were produced. Sections 2 to 4 below discuss the reports produced and the results of those studies. Each report is referenced at the start of the discussion regarding that report.

This report summarises the experimental programme undertaken on the release of liquid hydrogen and the conclusions drawn from this work regarding the safety aspects of the transport and storage of liquid hydrogen. The experimental investigations summarised in this report are:

- Experiments to investigate the mechanisms of the surface ignition, and minimum electrical spark ignition energies. These experiments utilised an in-plume, continuous ignition source.
- Experiments to investigate the effect of the substrates onto which liquid hydrogen could be spilled; the substrates of interest in this work were concrete, sand, water, and gravel. In addition to looking at the effect of the substrate, the ignition position and the ignition time from release were also investigated.
- Experiments undertaken to investigate the phase transitions of hydrogen and the surrounding components of air under cryogenic temperatures. Studies reported here investigated hydrogen in air condensed phase formation and the potential explosive risks of the condensed phase materials. This included the conditions required to support the formation of various compositions of liquid and solid condensed phase mixtures.
- Experiments undertaken to investigate the behaviour of a pool of liquid hydrogen when water from a sprinkler system or water hose was introduced.
- Experiments undertaken to investigate charge accumulation and static discharge potential including the propensity for liquid hydrogen to generate a static charge sufficient to cause ignition of a hydrogen cloud. Two distinct charging modes

were assessed, one from charge development within a multiphase hydrogen jet, and the other charge development on pipework containing liquid hydrogen.

Sections 2 to 4 below discuss the results reported as part of PRESLHY deliverable D4 for these experiments. The full experimental reports are available as part of this report series and only a summary of the outputs of each is given below.

2. Flammability properties of cryogenic mixtures

2.1. The influence of low temperature on the flammability limits of hydrogen gas (Proust, 2021)

During the PRESLHY experimental work for work package 4, the influence of cryogenic temperatures on the flammable limits was investigated. The equipment and experimental consideration of the spark system used to determine the flammability limits of hydrogen-air mixtures at various temperatures is described in detail in PRESLHY deliverable D4.4 (Proust, 2021). For all environmental conditions investigated, the resulting hydrogen flame was invisible to the naked eye and the ignition process was effectively silent. The results obtained during these experiments are presented in Table 1.

Temperature (°C)	LFL (% Hydrogen v/v)	UFL (% Hydrogen v/v)
20	5	70
-60	5.6	66
-120	6	60

Table 1: Lower flammable limit and Upper flammable limit of hydrogen-air mixtures as function of the temperature at atmospheric pressure (Proust, 2021)

Table 1 shows that as the temperature decreases the lower flammable limit increases and the upper flammable limit decreases. As the ambient temperature was reduced to -120°C the lower flammable limit increased by 1% vol/vol and the upper flammable limit decreases by 10% vol/vol.

2.2. The influence of concentration and temperature on the minimum ignition energy of hydrogen-air mixtures (Proust, 2021)

During the PRESLHY experimental work for work package 4 the minimum ignition energy of hydrogen was investigation under a variety of conditions. The experiments looked at the effect of temperature, in this case from ambient down to -130°C, for hydrogen-air mixtures while the concentration of hydrogen was varied between the flammable limits of 4 to 75%, to determine the minimum ignition energy. The experiments were limited to temperatures above -130 °C as this is the lowest that can be achieved in a jet of liquid hydrogen and air at the upper flammability limit.

The equipment and experimental considerations used to measure the minimum ignition energy using a continuous spark ignition source are described in detail in PRESLHY deliverable D4.4 (Proust, 2021). As spark ignition is an instantaneous process, the effective time scale of the ignition period negates any flow effect and therefore the flow can always be considered to be 0 ms^{-1}. The subsequent spreading of the initial flame kernel to the rest of the flammable cloud is a flame propagation phenomenon and not a flow phenomenon.

It was found that at atmospheric temperature a minimum ignition energy of 18 µJ was seen at a concentration of 20% hydrogen in air, this is in line with the literature values as discussed in detail in PRESLHY deliverable D4.1 (Lyons, et al., 2020). The ignition process was also observed to have a small energy overlap boundary, energies below this boundary fall into the ‘no ignition zone’ and energies above this boundary fall into the ‘ignition zone’. As would be expected, ignition energies within the overlap boundary can

lead to an ignition but ignition is not always achieved. Proust observed that in these experiments the energy overlap boundary was found to be a factor of 2, whereas he quotes the previous studies suggested that the overlap boundary was closer to a factor of 10. To calculate the high voltage spark energy, the voltage breakdown was measured and found to be 2700 V in air at ambient temperature and atmospheric pressure. Results for these experiments can be found in Figure 1 (for ambient temperature) and Figure 2 (for -100°C) where the energies quoted are those stored in the capacitors prior to discharge.

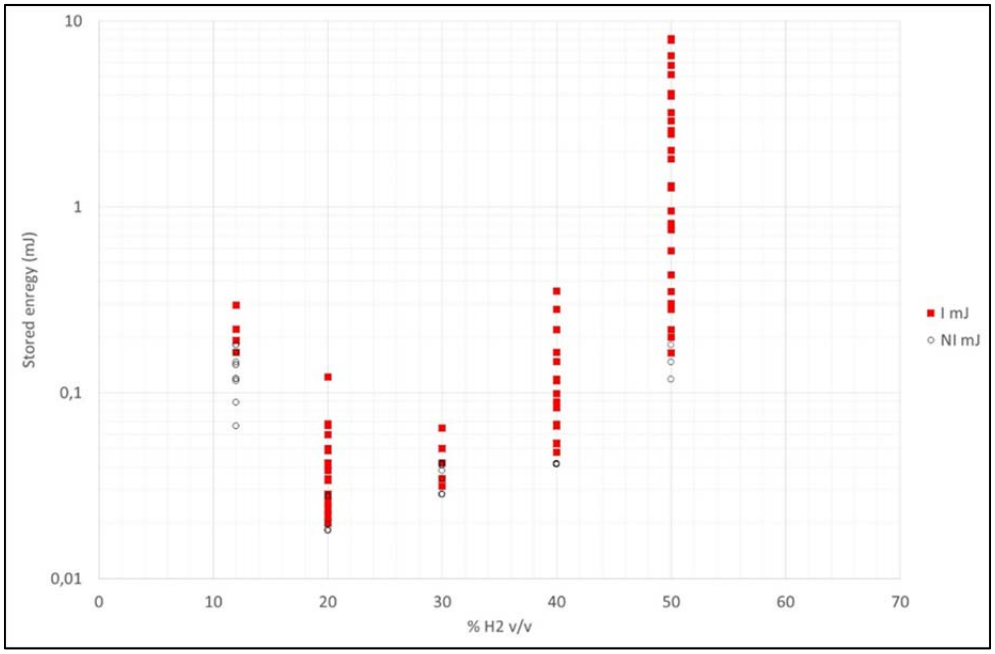

Figure 1: Minimum ignition energy for hydrogen-air mixtures at ambient temperature and atmospheric pressure (Proust, 2021)

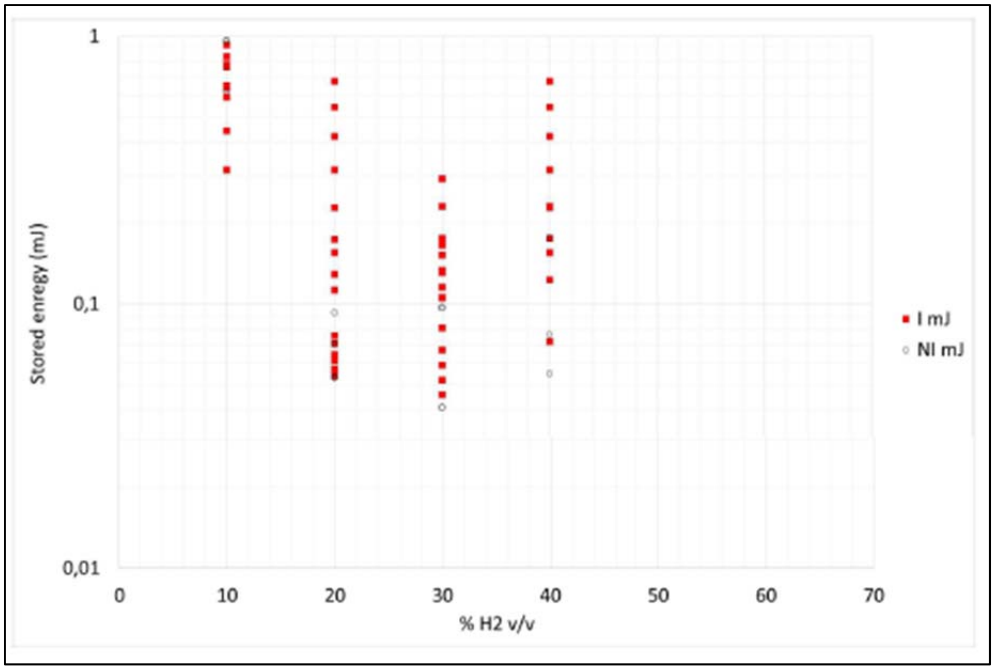

Figure 2: Minimum ignition energy for hydrogen-air mixtures at -100°C and atmospheric pressure (Proust, 2021)

It was found that at -100°C the minimum ignition energy of 50 µJ was seen at a concentration of 30% hydrogen in air; separate assessments identified that the breakdown voltage in the air at this temperature and at atmospheric pressure was found to be 3500 V. Throughout it was found that sub-ambient test results proved more difficult to reproduce and as a result the results were found to be less precise than at ambient temperatures.

A systematic investigation into the evolution of the minimum ignition energy as a function of the temperature at a composition of 20% hydrogen in air, was also performed. First, the breakdown voltage variation of dry air as temperature was investigated to find a baseline figure: It was found that there was an inverse relationship between breakdown voltage and temperature, in that the breakdown voltage increased as the temperature decreased, see Figure 3.

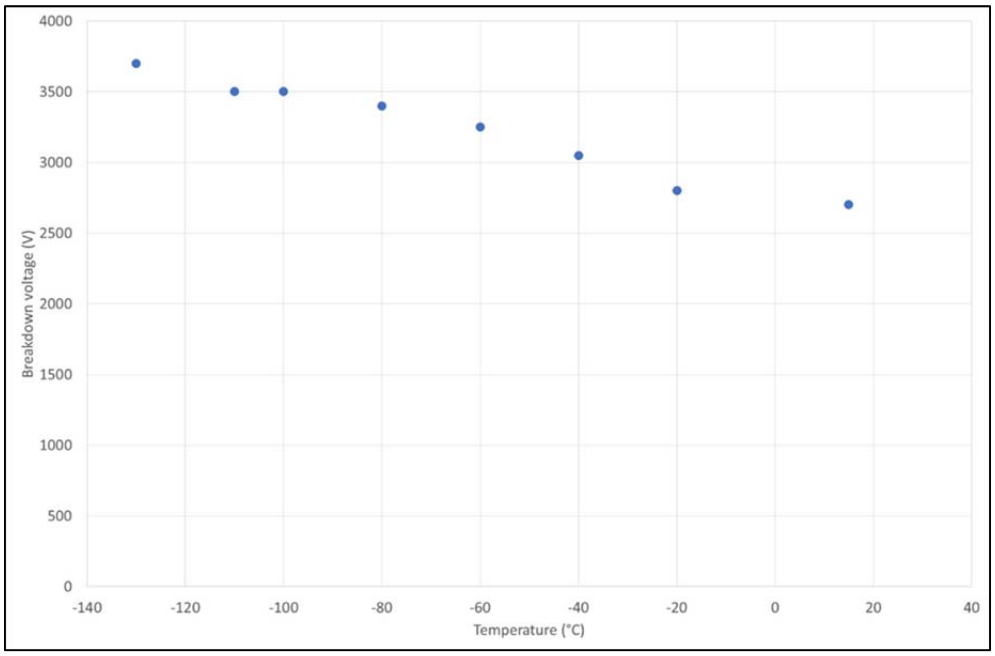

Figure 3: Breakdown voltage in the air as function of the temperature at atmospheric pressure (Proust, 2021)

Then the evolution of the minimum ignition energy for the composition of 20% hydrogen in air was investigated as a function of the temperature. Within these trials, the minimum ignition energies generally increased as the temperature decreased.

2.3. The influence of concentration, temperature, and flow velocity of hydrogen on the critical hot surface ignition temperature of hydrogen-air mixtures (Proust, 2021)

During the PRESLHY experimental work for work package 4 the critical hot surface ignition temperature was investigated under a variety of conditions. The experiments determined the critical hot surface ignition temperature under the effect of:

a) Flow velocity (0 to 30 ms^{-1});
b) Temperature (ambient to -130°C)

for hydrogen-air mixtures while the concentration of hydrogen was varied between the flammable limits of 4 to 75%. The experiments were limited to -130 °C as this was determined to be the lowest that can be achieved in a jet of liquid hydrogen and air at the upper flammability limit (Proust, 2021).

The equipment and experimental considerations used to measure the hot surface temperature are described in detail in PRESLHY deliverable D4.4 (Proust, 2021).

The critical hot surface temperature was determined to be close to 600°C (at all concentrations utilized); this value was very close to the autoignition temperature (Proust, 2021). This does not vary with the concentration of hydrogen and, given the uncertainty of the measurement of the temperature of the hot coil, the influence of the concentration of hydrogen, and therefore the reactivity of the mixture, seems very small, as shown in Figure 4.

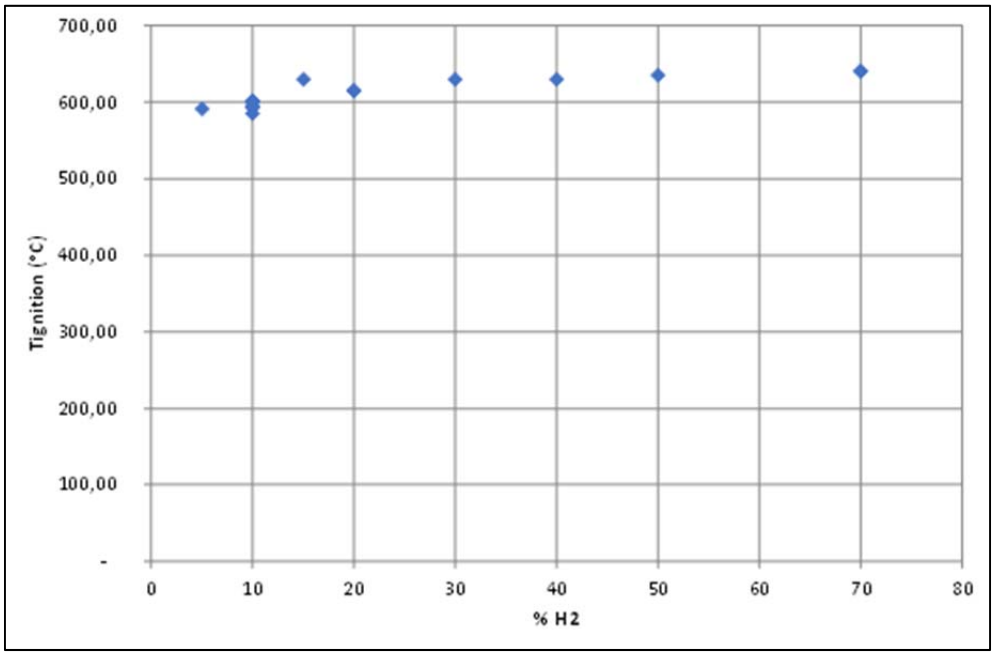

Figure 4: Influence of the proportion of hydrogen in the mixture on the hot surface ignition temperature (ambient conditions and at rest) (Proust, 2021)

Figure 4 shows that for a mixture of 10% hydrogen in air the hot surface ignition temperature was the lowest and experimentation showed the ignition event to be clearly defined. This flammable mixture concentration was chosen to investigate the influence of temperature on the hot surface ignition temperature. To achieve flexibility of the composition of the atmosphere and its temperature, gaseous nitrogen, gaseous oxygen, gaseous hydrogen, and liquid nitrogen were injected via calibrated ports in the flange of the pipe. There was no detectable difference in sample response given the measurement uncertainties, which was in line with the predictions, as discussed by Proust, Figure 5.

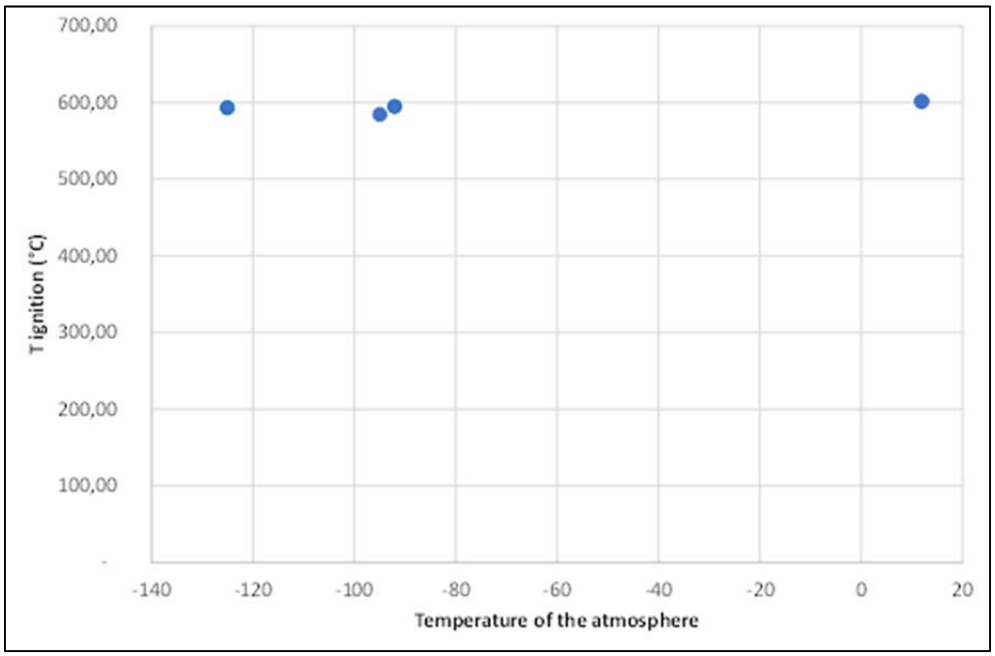

Figure 5: Influence of the temperature of the hydrogen-air mixture on the hot surface ignition temperature (10% hydrogen at rest) (Proust, 2021)

It was found that for a mixture of 10% hydrogen in air at ambient conditions the influence of the velocity of the flammable atmosphere was negligible and less than postulated by Proust, Figure 6.

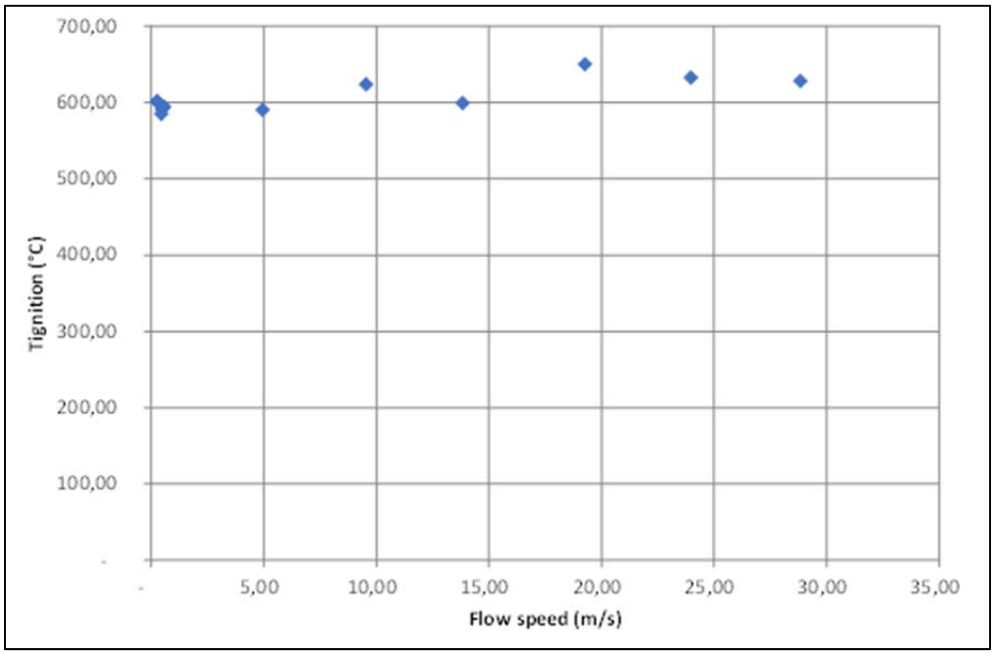

Figure 6: Influence of the velocity of the hydrogen-air mixture on the hot surface ignition temperature (10 % hydrogen, ambient conditions) (Proust, 2021)

3. Environmental considerations and interactions regarding cryogenic hydrogen

3.1. The influence of surface substrate on the ignition and combustion behaviour of cryogenic hydrogen pools (Friedrich, Veser, Gerstner, Kuznetsov, & Jordan, 2021)

During the PRESLHY experimental work for work package 4 the influence of the surface substrate on the ignition and combustion behaviour of liquid hydrogen pools was investigated. The equipment and experimental considerations used to investigate the effect of the surface substrate are described in detail in PRESLHY deliverable D4.7 (Friedrich, Veser, Gerstner, Kuznetsov, & Jordan, 2021). Substrates investigated in this work were concrete, sand, water, and gravel. The other parameters varied in the tests were the ignition position and the time given for the hydrogen to interact with the substrate before ignition. The variations in ignition position and ignition time were made on the basis of hydrogen in air concentration data determined from unignited tests in which hydrogen concentrations were measured in different heights for different filling levels of the pool. The effect of these variations on ignition and combustion behaviour was then assessed by attempting to ignite the flammable atmosphere above the pool.

To get reproducible initial conditions for the experiments, the pool was filled twice prior to the ignition initiation. This procedure allowed sufficient pre-cooling of the substrate so that it was possible to obtain reliable information on the filling level.

The experiments showed that gravel demonstrates some unique behaviour when compared to the other substrates investigated. Due to the surface substrate high porosity, the liquid hydrogen can pool and collect within the gaps between the gravel, it consumes much higher quantities of liquid hydrogen until a pool forms above the substrate surface. However, once the pool above the substrate has evaporated, the now cold substrate starts to condense and freeze out components of ambient air that then accumulate in the free space between the substrate particles. If ignition of a hydrogen in air mixture is achieved above the pool, these condensed air components vaporize again and reinforce the loads of the explosion observed.

3.2. The influence of solid depositions of air on the flammability of cryogenic hydrogen (Atkinson, 2020)

During the PRESLHY experimental work for work package 4 the influence of solid deposits of air, deposited on the ground during a liquid hydrogen release at ground level, on the flammability of liquid hydrogen was investigated. The equipment and experimental considerations used to investigate the formation and behaviour of solid air deposits is described in detail in PRESLHY deliverable D4.8 (Atkinson, 2020).

This work was based on data reported in the literature, HSE research reports RR986 (Royle & Willoughby, 2014) and RR987 (Hall, 2014); these reports describe experiments on unignited and ignited low pressure (1 bar) jets of liquid hydrogen respectively, these data indicating that trial-to-trial results varied considerably. In the report by Hall the majority of test resulted in what was described as a soft report, followed by a low rumble, and a gentle jet flame was then observed issuing from the hydrogen release pipe. The flame speeds measured from the high-speed video were found to develop up to 50 m/s, dependent on the ignition conditions (Hall, 2014). IR footage also showed that the extent of the flammable cloud was similar to the visible water vapour cloud, created by the very

cold hydrogen cloud. In one of the tests reported by Hall a detonation event was observed. In PRESLHY deliverable D4.8 Atkinson undertook an investigation into the conditions and scenario that resulted in that detonation.

The test in question resulted in a deflagration to detonation transition event occurring. This event occurred after the release of liquid hydrogen and the subsequent accumulation of solids at ground level for 260 seconds. The event detonation center was adjacent to the condensed solid and therefore Atkinson investigated the composition of the condensed solid phase to determine if this contributed to the detonation event. As part of this investigation Atkinson proposed the following mechanism for the production of solid deposits.

The initial part of the mechanism involves the components of air being condensed by gaseous hydrogen formed as the liquid hydrogen is vaporised due to thermal contact with the ground and entrained air. The vaporisation removes energy from the surroundings, so resulting in condensation.

After this initial cooling period of the overall system, the main source of heat input to liquid on the ground comes from entrained air. This heat input is in the form of direct contact with air, or gaseous hydrogen, and leads to deposition of droplets and crystals of condensed air into the liquid. Deposited crystals of solid air are then transported by the liquid flow, coming to rest where the liquid flow is sufficiently shallow and slow. Some deposition of air occurs beyond the edge of the liquid hydrogen flow and this adds to the mass of solid air formed, whilst also raising its temperature above the boiling point of hydrogen. This leads to moderate levels of oxygen enrichment occurring during the condensation of air. The temperature and chemical composition of solids formed from releases of liquid hydrogen are likely to vary significantly with environmental conditions. Low relative speeds between gaseous hydrogen and air could also allow buoyancy stabilisation of a condensation zone where the temperature was close to the initial boiling point of air and the condensed material was oxygen rich.

Figure 7 shows a schematic of how the initial growth of a solid deposit might proceed.

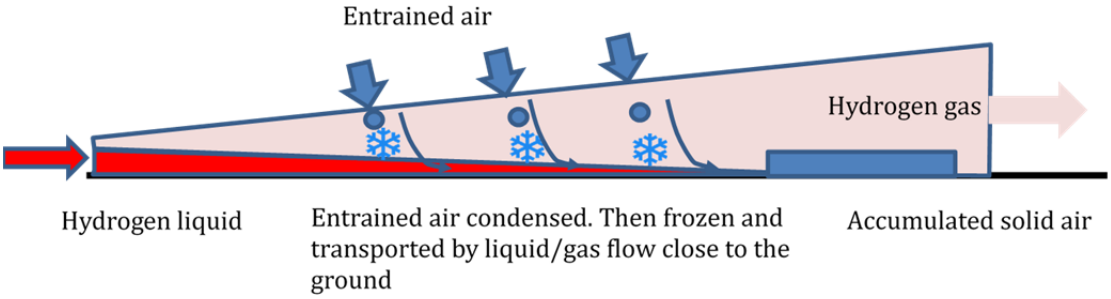

Figure 7: Schematic showing how solid deposits accumulate (Atkinson, 2020)

This mechanism is supported by the observed and calculated results, explained below.

In the experiment by Hall, it was found that the amount of solid deposited in the test would have been approximately 17 +/- 5 kg. It was also calculated that to account for the heat released during the detonation event, 3.7 Kg of the solid deposit must be attributed to solid phase oxygen, with the rest consisting of other constituents of air that were not considered to be involved in the detonation event. It was determined that the heat transfer from the ground accounted for around 35% of the liquid hydrogen vaporized in the

experiments, leaving the remaining 65% available to undergo heat transfer with the air to produce a condensed phase of air components. A release of 35.1 kg of liquid hydrogen would therefore have to have an overall efficiency greater than 50% for 17 kg of solid air deposits to be formed. Table 2 shows the maximum yields in this case.

Composition (mole % Oxygen)	Final temperature (K)	Total solid (kg)	Oxygen (kg)
21	20 (boiling point of hydrogen)	14.8	3.5
21	58 (melting point of condensate)	31.6	7.4
44	20 (boiling point of hydrogen)	7.5	3.6
44	52 (melting point of condensate)	13.8	6.6

*Table 2: Calculated maximum quantities of solids (air and oxygen-rich air) that can be produced from 35.1 kg of liquid hydrogen, assuming an efficiency of **50%** (Atkinson, 2020)*

In the oxygen-rich cases, where oxygen composition in the condensate was a mole factor of 44%, lower solid yields were calculated. In these cases, approximately 30% of the air condenses to form a solid. Excess cold, nitrogen-rich gas would also be produced which requires the vaporisation of large amounts of liquid hydrogen but does not contribute to the accumulated solid. The height profile of the mass of the observed solid at the end of the flow is also consistent with this mechanism. Moving back from the front, the depth of solid appears to increase, which would correspond to the continued deposition beyond the limit of liquid flow. This suggests that towards the end of the test, most of the solid mass would have been significantly above the boiling point of hydrogen. However, solids right at the front of the mass would have still been in contact with liquid hydrogen.

However, there are still questions regarding this mechanism such as with regards to the energy balance calculations, if all the solid deposited was at some point cooled to liquid hydrogen temperatures, then tight limits on the possible production of solid masses apply and the observed high yields of observed solid remain to be explained.

In the trials by Hall in which a secondary explosion was observed, the large quantity of solid observed means only a small proportion could have been both significantly oxygen-enriched and cold enough to trap sufficient liquid hydrogen within the solid mass in order to form an intimate mixture.

During the immediate post-ignition phase of the hydrogen in air cloud ignition, above the liquid hydrogen and solid condensates, the liquid hydrogen weakly absorbs the thermal radiation produced: With this level of absorption it is likely that the jet fire does not prevent contact between a ground level flow of liquid hydrogen and accumulated solid air. On contact with the thermal radiation, large quantities of solid air melt rapidly and become volatile. Regression rates of the solid surface were calculated to be several mm per second (Atkinson, 2020). This leads to oxygen enrichment of the atmosphere around the melt to a possible level of around 70% mol/mol. This is the most likely phase change mechanism that led to the formation of the volatile hydrogen in air mixture responsible for the observed secondary explosion seen in the test described by Hall. The solids would also have probably contained a small proportion of condensed water. This might have significantly increased their potential to absorb thermal radiation after ignition.

The ground level jet releases of liquid hydrogen in a wide range of circumstances may allow the accumulation of a mixture of condensed air and hydrogen with a composition that has the potential to form an explosion hazard. This hazard mechanism must be

considered as part of a risk assessment process for such events alongside jet fire and vapour cloud explosions.

More experimental and modelling work to investigate the mixing and deposition of solid air during contact with cryogenic hydrogen is required. It would be particularly important to know how the risk is affected with the scale of release.

3.3. Interaction between pools of accumulated cryogenic hydrogen with water sprays and jets (Atkinson, 2020)

During the PRESLHY experimental work for work package 4 the interaction of pools of liquid hydrogen with water spray and jets was investigated. These experiments consisted of either a fine spray of water being discharged from a spray nozzle above a pool of liquid hydrogen, or a jet of water being discharged directly downwards into a pool of liquid hydrogen. The equipment and experimental considerations used to measure the interaction of liquid hydrogen with a water spray are described in detail in PRESLHY deliverable D4.8 (Atkinson, 2020).

It was found for the test conditions, both the water spray and jet, that contact between water and liquid hydrogen will not necessarily cause a rapid phase transition; however this does not rule out such energetic events occurring under other circumstances. It was not possible to determine, or investigate, all the factors that could lead to the occurrence of a rapid phase transition as this is not very well understood in the literature.

The results were able to demonstrate that, although the exact conditions are at present underdefined, emergency water spray suppression through sprinklers and monitors (water jets) can be used to control the flow or accumulation of liquid hydrogen without risking the occurrence of a rapid phase transition. This activity does however lead to an increase in the rate of vaporisation and therefore if the resulting hydrogen-air mixture were to be ignited there could be a larger initial fireball than would have been produced without water spray suppression.

4. Charge generation and accumulation in cryogenic hydrogen

4.1. Electrostatic charging and ignition of multiphase jets

During the PRESLHY experimental work for work package 4 the electrostatic charging and ignition of multiphase hydrogen jets was investigated. The equipment and experimental considerations used to measure the charging and discharging are described in detail in PRESLHY deliverable D4.6 (Lyons & Hooker, 2020). A full assessment of the electrostatic measurement methods considered and the rationale for adopting those that were used can be found in PRESLHY deliverable D4.1 (Lyons, et al., 2020). Some of the measurements were taken during the rainout experiments, summarised in work package PRESLHY deliverable D3.6 (Lyons, Coldrick, & Atkinson, 2020).

Two distinct modes of electrostatic charging in liquid hydrogen releases from steel pipework were investigated: the charging due to charge separation near to the liquid hydrogen-pipe interface; and the charged cloud generated by a jet of hydrogen, which may be liquid, gaseous or two-phase, and may also contain condensed solids from air.

4.1.1. Charged cloud generated by a jet of cryogenic hydrogen (Lyons & Hooker, 2020)

Measurement made in these experiments indicated that the multiphase hydrogen jet itself does not create a significant charge, but interactions with the air can cause intermittent spikes in field strength. In particular, air in the pipework being ejected and solidified air forming around the release point, subsequently breaking off and flowing downstream, appeared to be the cause of the electrical fields measured in these experiments. These effects could vary with different initial conditions either at the nozzle or in the tanker.

As described in PRESLHY deliverable D3.6 (Lyons, Coldrick, & Atkinson, 2020), the interaction between the jet formed from a cryogenic release of hydrogen and the air produces phase changes in the components of air. Of particular relevance to these investigations is the formation of a solid cone around the release point, which affected the flow of the jet in some cases. These solid deposits cyclically formed and broke off during the releases with 6 and 12 mm diameter nozzles, but not with a 25.4 mm diameter tanker nozzle.

Experiments were carried out to measure the electrical field of a plume of cryogenic hydrogen, and no significant plume measurements were obtained in five of seven trials, the other two showing intermittent spikes of 100-140 Vm^{-1} through the release.

In one of the two experiments where intermittent charge spikes were detected (trial 5 of the test program) both initial and mid-flow peaks were observed; these measurements were made using a free-standing field meter setup 0.5 m from the centreline of the jet and 0.5 m from the release point: Figure 8 shows the results. For this trial, the tanker pressure was a nominal 1 barg and a 25.4 mm nozzle was used. It can be seen from the pressure plot in Figure 8 where the release began and ended.

In the other experiment (trial 7) that showed intermittent charge spikes, a Faraday pail was utilised with the field meter closer to the centreline of the jet at 0.125m. A peak was observed at the initial point, shown in Figure 9.

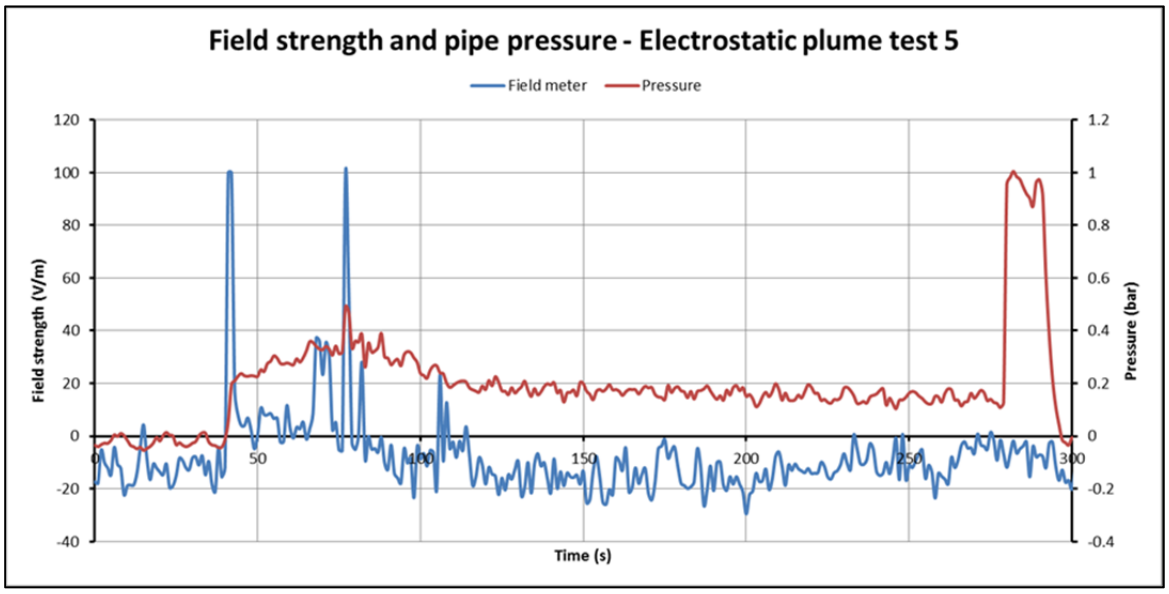

Figure 8: A graph of field strength and pipe pressure for trial 5 (Lyons & Hooker, 2020)

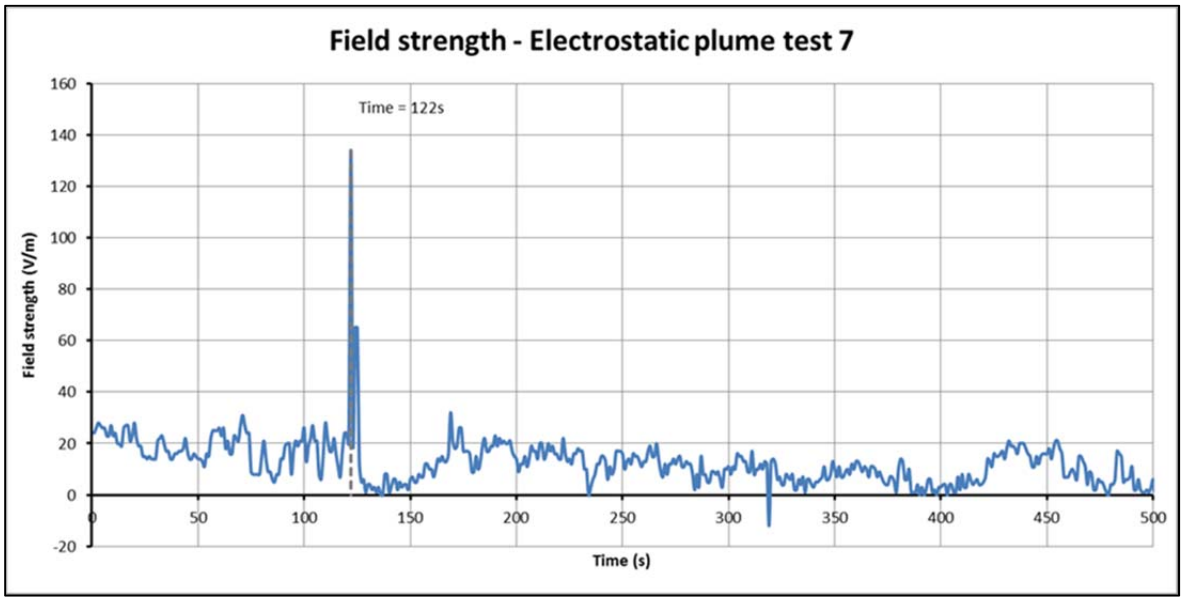

Figure 9: A graph of field strength for trial 7 (Lyons & Hooker, 2020)

In trial 7 in order to determine if the initial peak of hydrogen was charged, the release was halted, and venting began multiple times throughout the trial. Despite multiple initiations through the main release point, only one spike in field strength was observed. This initial spike in field strength seen in both experiments corresponds with the initiation of the release. Since only two of the trials showing identifiable fields in the plume, it can be suggested that cryogenic hydrogen releases at relatively low pressures (maximum of 5 barg), do not reliably generate an electric field under the conditions of the experiments.

For both trials that obtained positive results, a spike of 100-140 Vm^{-1} was recorded as the flow was first initiated. Since the initial spikes correlated with the opening of the release valve it is thought unlikely that hydrogen generated the charge, but rather the air in the final 1.75 m section of unpurged pipework being ejected in a turbulent manner. This hypothesis is supported by the results of trial 7, which contained multiple initiations of the release during the trial as the operation was changed from venting to a main release

three times, with only the initial one showing the spike in field strength. After this initial venting procedure, during the subsequent venting stages of this trial, cryogenic hydrogen was still present in the pipework and would be expanding out of the main release point as it warmed, causing a slightly positive pressure and meaning air entrainment back into the pipework was unlikely, therefore no charge was generated upon the re-initiation of the release.

The lack of this phenomenon being observed in the other trials could be due to either

i) no field being generated due to insufficient levels of air or turbulence in the release, or
ii) the measurement device being too far away to register the small and transient charge as positive results were only obtained with the field meter close to the release point.

Based on the 5% accuracy of the field meter, the field at the larger distance (0.5 m) would have been less than ca. 5 V/m on the 100V/m range in order to have not registered as a significant reading. This means that the field that would have registered at the closer position of 0.125 m (i.e. when the Faraday cage was in use) under those conditions would have been less than 20 V/m, since the field would drop off in proportion to the reciprocal of the distance for a nominally cylindrical jet or plume. Therefore, the undetected fields at the larger distance would not have been greater than the largest field registered at the closer distance and subsequently used in the assessment of the hazards (see section 4.1.3 below).

The other anomalous result was the secondary spike and corresponding pressure increase in trial 5. While not confirmed, this secondary spike and rise in pressure was proposed to have been caused by a phase change in the air around the nozzle creating a cone of solid air impinging on the flow and subsequently breaking off and registering a charge with the field meter.

From these plume measurements, it can be said that while a transient field can be measured, a charged plume forming from an established cryogenic jet is unlikely for the initial conditions within the scope of these experiments.

4.1.2. Charging due to charge separation near to the cryogenic liquid hydrogen and pipe interface (Lyons & Hooker, 2020)

Measurements made in these experiments demonstrated that it was possible for liquid hydrogen to induce a current on a section of electrically insulated pipework. This charging mechanism is a complicated function of the phase of liquid hydrogen in the pipework, the turbulence of the flow, and the resistance to ground of the section of the pipework. Frost formation on the outside of the pipework dynamically changed the resistance to ground throughout each trial, making the subsequent interrogation of the results more challenging. The resistance to ground of the electrically isolated section of pipework was measured throughout each test day to help with the analysis of the results. It should be noted that the input impedance of the electrometer used is orders of magnitude lower than the resistance to earth of the isolated pipe section as so the measured currents should not have been adversely affected.

It was found that a charge was not reliably generated in the pipework and when a charge was measured, the full extent is often not known due to the measurement device over-ranging. In no cases where the electrometer was on the 200 μA range did the current exceed this value.

One factor found to influence the results was the build-up of frost on the electrically isolated pipework section. Once the frost had developed the resistance measurements were orders of magnitudes lower, typically around 10^4 Ω with frost rather than 10^7 Ω without, which would limit the amount of current generation by causing a larger leakage rate. The balance between the charge generation from the action of the process fluid on the pipework and the leakage to earth results in the measured the wall current, which is thus heavily dependent on the resistance to earth of the pipework. This makes the interpretation of the results difficult as the resistance changes dynamically through the trials due to the formation of frost, reducing the resistance to earth. Due to the experimental setup, it was only possible to take resistance measurements between trials and therefore only give an indication of the value at the end of the trial (ie once frost formation had peaked). For the trials with an indicated value in the order of 10^4 Ω it is possible that charge generation is occurring during fluid movement, but at a rate insufficient to overcome the leakage to earth.

In some experiments the wall current rose sharply part way through the experiment and went above the maximum range of the electrometer. The wall current, temperature and mass flow rate graphs for one trial, trial 8, are shown in Figure 10.

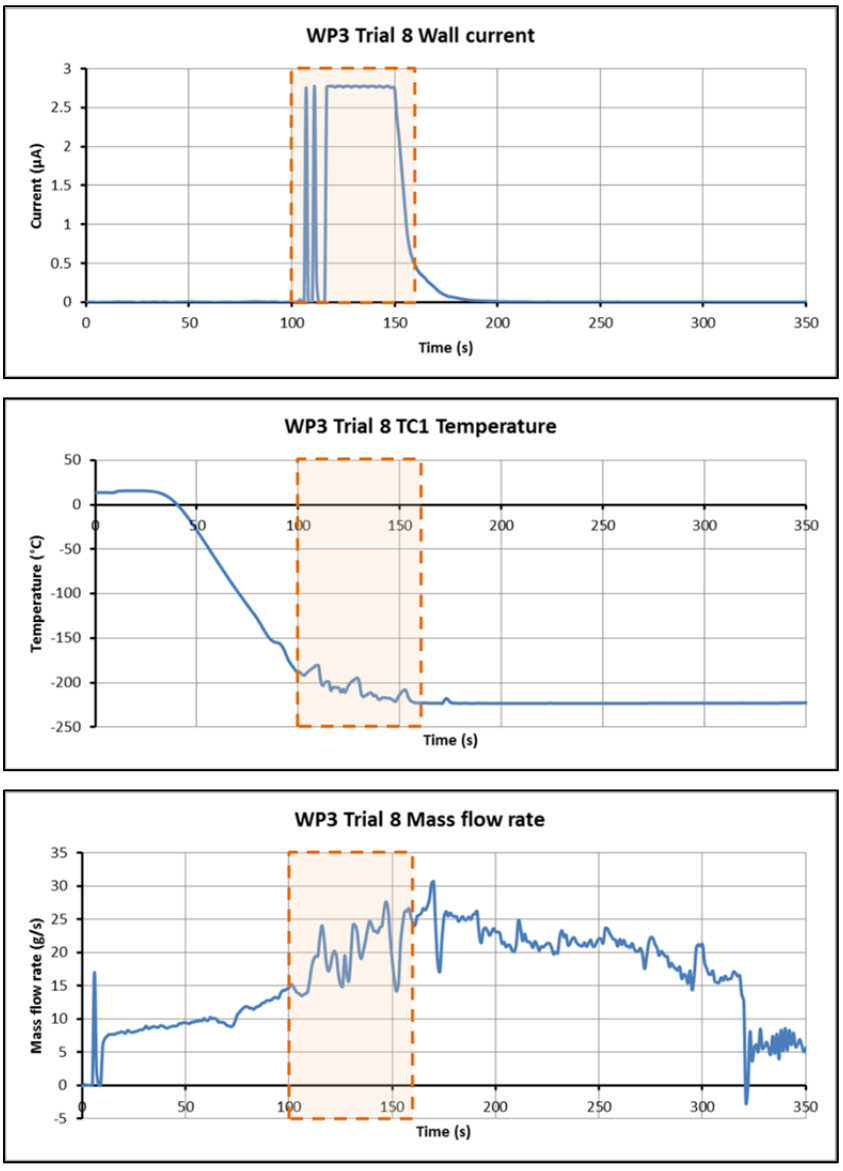

Figure 10: Wall current, temperature, and mass flow rate results for WP3.5 trial 8 (Lyons & Hooker, 2020)

In Figure 10 the wall current measured from the electrically insulated pipe is shown. The temperature and mass flow rate graphs indicate the phase of the fluid. The temperature sensor is located before the electrically isolated pipe and the mass flow meter after.

The temperature graph is representative of the results for all trials carried out and contains three distinct regions.

i. 0-100 seconds: The initial smooth reduction in temperature, a single-phase gas flow,
ii. 100-160 seconds: An oscillatory reduction in temperature, a two-phase flow,
iii. 160-350 seconds: A final steady state, a full liquid flow.

From the figure it can be seen that charge generation consistently fell within the two-phase flow region of the graph. It can also be shown that the mass flow meter was unable to resolve two-phase flow, resulting in the unstable output shown. This unstable region can also be seen to correlate well with the charge generation. It is postulated that the primary mode of charge generation during these experiments is the kinetic energy transferred from a roiling two-phase flow to the surrounding pipework, which is supported in previous work by Cassutt et al (Cassutt, Biron, & Vonnegut, 1961) whereby charge generation was observed as being most significant during two-phase flow.

An extension of this mode of charge generation is that any initial condition that encourages or extends the two-phase flow will also cause more charge generation. This includes the initial state of the pipework being relatively warm; additional heat transfer into the process fluid will result in a higher degree of vaporisation and two-phase flow at the interface. Other initial conditions that affect the phase of the fluid in the pipe are the tanker pressure and the release nozzle size. It was observed that 5 barg releases had a higher volumetric flow rate than those of 1 barg therefore decreasing the time required for the pipework to cool (and thus, reducing the period of two-phase flow). Trials using a 25.4 mm nozzle were similar for all releases in that a predominantly liquid flow developed quickly, even during the 1 barg releases. Conversely, the choked flow of 6 mm nozzles produced a significant back pressure, extending the latency of the hydrogen in the pipe, resulting in a higher level of gaseous flow rather than a turbulent two-phase flow (thereby reducing charge build-up).

From these trials it is evident that the flow of liquid hydrogen in pipework can cause electrostatic charging and that certain conditions encourage it. The applications of these findings revolve around either designing liquid hydrogen pipework so that the development of two-phase flow is limited (such as through vacuum insulation), or by ensuring that the pipework contains no electrically isolated sections.

While occasional spikes in field strength were observed within multiphase hydrogen jets that forms during a release of liquid hydrogen, the plume itself did not become charged. These transient spikes have been attributed to entrained air, either in the form of air in the pipework being ejected or complex phase changes around the release point causing solids to flow downstream.

Liquid hydrogen flowing in electrically insulated pipework was also shown to generate a charge. This occurs from the action of a turbulent two-phase flow on the surrounding pipework. Initial conditions that encourage a turbulent two-phase flow also encourage charge generation in the pipework. For ground-based applications, electrical continuity between the pipework and earth is important to avoid charge build-up.

The experiments suggested that electrostatic charges may pose a credible hazard when considering liquid hydrogen facilities, and this is discussed further in Section 4.1.3. The charging, however, does not appear to be significant during single phase liquid or gaseous flow. Significant charging does occur during two-phase flow, and on the substances or objects that the hydrogen interacts with, such as condensed ice or air. For a fixed facility, maintaining continuity to earth and paying attention to objects in the potential path of a release, would limit the likelihood of electrostatic charging and therefore limit the hazard.

4.1.3. Hazard Analysis (Lyons & Hooker, 2020)

The results reported in Sections 4.1.1 and 4.1.2 can be used to carry out an assessment of the ignition hazards presented by the formation of charged jets / clouds and charging of pipework due to liquid hydrogen flow in the case of a release.

The potential sources of electrostatic ignition that are of interest in this case are,

a) Corona discharges,
b) Sparks from pipes or other plant items,
c) Lightning discharges directly from within any cloud formed, and
d) Sparks from other conductors.

Knowledge of the electric field at any point in a release within a Faraday cage allows the charge density of the cloud to be estimated using Equation 1: an assumption is made that a uniform charge density exists within the cylindrical Faraday cage.

Equation 1

$$\sigma = \frac{2\varepsilon_0 \varepsilon_r E}{R}$$

Where σ = charge density within the cloud (C m^{-3})

ε_0 = permittivity of air (ca. 8.85 x 10^{-12} F m^{-1})

ε_r = relative permittivity of the cloud, which will be approximately = 1

E = the electric field (V m^{-1})

R = radius of the cage (m)

Using the maximum measured field within the experiments discussed in Section 4.1.1, which was found to be 140 V m^{-1}, the charge density in the cloud during that experiment can be estimated to be 2.0 x 10^{-8} C m^{-3}.

These values of electric field and charge density can be used to assess the effect of the potential ignition sources listed above within the liquid hydrogen release. These are discussed in the following sections.

a) Corona discharges

The onset of corona discharges cannot be ruled out even for such low electric fields (i.e. similar strength to normal atmospheric fields). However, it has been observed (Hooker, Royle, Gummer, Willoughby, & Udensi, 2011) that corona currents of in excess of a hundred microamps are required to cause ignition of hydrogen, even at ambient temperature, and that a potential of 20 kV was required.

b) Sparks from pipes or other plant items

The resistance to earth required to avoid hazardous potentials can be derived from the current measurements made on the pipe section, using ohms law (Equation 2).

Equation 2

$$R = \frac{V}{I}$$

Where R = resistance (Ω)

V = potential considered hazardous (V)

I = charging current (A)

A value of 100 V is conservatively used for a hazardous potential in this case (British Standards Institution, 2013). Taking a pessimistic value of 200 x 10^{-6} A for the charging current (actual measured currents during experimentation were significantly less than this, but a higher value has been applied to allow for higher charging currents from longer lengths of piping) this gives a maximum resistance requirement of 0.5 x 10^{-6} Ω (or 0.5 MΩ) to mitigate against spark discharge. Such resistance levels should be readily achievable for conducting pipes, plant items and hoses. International guidance for avoiding electrostatic hazards (British Standards Institution, 2013) gives maximum values of resistance to earth of 10 Ω for metal items and 10^{-3} Ω for conductive hoses.

c) Lightning type discharges directly from the cloud or jet

This type of discharge can occur from a charged cloud of droplets or particles if the electric field at the edge of the cloud is large enough. A field strength of more than 500 kVm^{-1} is reported as being required (British Standards Institution, 2013). Clearly this precludes the occurrence of a lightning type discharges, at the scale used in PRESLHY, where a maximum field of only 140 kV m^{-1} was obtained.

The size of a cloud required to potentially cause lightning discharges can be estimated from the charge density value using Equation 3.

Equation 3

$$\frac{E\varepsilon_0\varepsilon_r}{\rho} = r$$

Where r = radius of charged cloud (m)

E = electric field (i.e 500 kV m^{-1} for lightning discharges)

ε_0 = permittivity of free space, 8.85 x 10^{-12} F m

ε_r = relative permittivity of the cloud (being approximately 1)

ρ = cloud charge density (C m^{-3})

Using this relationship it can be shown that for a cloud with charge density of 2.0 x 10^{-8} C m^{-3} (the value calculated using Equation 1 from a maximum measured field of 140 V m^{-1} above) the cloud would need to have a radius of 220 m to support lightning-type discharges. This size of cloud has not been observed for the releases carried out for PRESLHY (which were typically a few meters in diameter) and it is apparent that it would take a large scale catastrophic event to have any chance of a lightning discharge occurring.

d) Sparks from other conductors

It is conceivable that, in some cases, the transient spikes in electric field were caused by a single, electrically isolated charged object. Consideration of the small electric field can be achieved by application of Equation 4.

Equation 4

$$Q = 4\pi E \boldsymbol{\varepsilon_0 \varepsilon_r} r^2$$

Where Q = charge on the object (C)

E = electric field (V m^{-1})

ε_0 = permittivity of free space, 8.85 x 10^{-12} F m

ε_r = relative permittivity of the cloud (being approximately 1)

r = distance from the charged object (m)

Using a value of 140 V m^{-1} as determined during and the experimental setup distance of 0.125 m gives a charge of less than 1 nC. A value of 10 nC is quoted as being required for the ignition of hydrogen (British Standards Institution, 2013). This indicates that the predicted charge of 1 nC on the object would be too small to be capable of igniting hydrogen.

In summary, the potential for electrostatic ignition as a result of accidental releases at up to 5 bar appears low providing plant and pipework are correctly earthed.

4.2. Electrostatic charging and ignition in hydrogen pools

During the PRESLHY experimental work for work package 4 the electrostatic charging and ignition of pools of liquid hydrogen was investigated. The equipment and experimental considerations used to measure the charging are discussed in detail in PRESLHY deliverable D4.5 (Friedrich, Veser, & Jordan, 2020). A full assessment of the electrostatic measurement methods considered and the rationale for adopting those that were used can be found in PRESLHY deliverable D4.1 (Lyons, et al., 2020).

4.2.1. High pressure, up to 200 bar, and moderate gas temperature, down to 80 K, experiments (Friedrich, Veser, & Jordan, 2020)

The first series of experiments discussed utilised gaseous hydrogen released from a reservoir and were performed at various temperatures, from ambient down to approximately 80 K and at reservoir pressures up to 200 bar. Besides the discharge characteristics and the transient jet behaviour, the electrostatic fields generated were also recorded to understand potential mechanisms for spontaneous ignition.

Cold jets at approx. 80 K were found to generate strong electrostatic fields, but no test showed a spontaneous ignition. The observed charge seems to be generated by ice crystals breaking off the nozzle and entering the hydrogen flow, these ice crystals were seen to form on the release nozzle before the tests.

Strong electrostatic fields, around 6000 V m^{-1}, were observed for the 80 K cold releases. They are typically 100 times larger than the fields measured for corresponding releases at ambient temperature. During these experiments it was observed that,

i) The signal at the field mill close to the release point (notated as FM1) is always stronger (of greater magnitude, ignoring polarity) than the signal recorded by the field mill at a larger distance (notated as FM2),
ii) Although the signal shows initially synchronous behaviour, the direction of the field vector is opposite,
iii) The maximum field strength increases with the reservoir pressure.

These effects are shown in Figure 11.

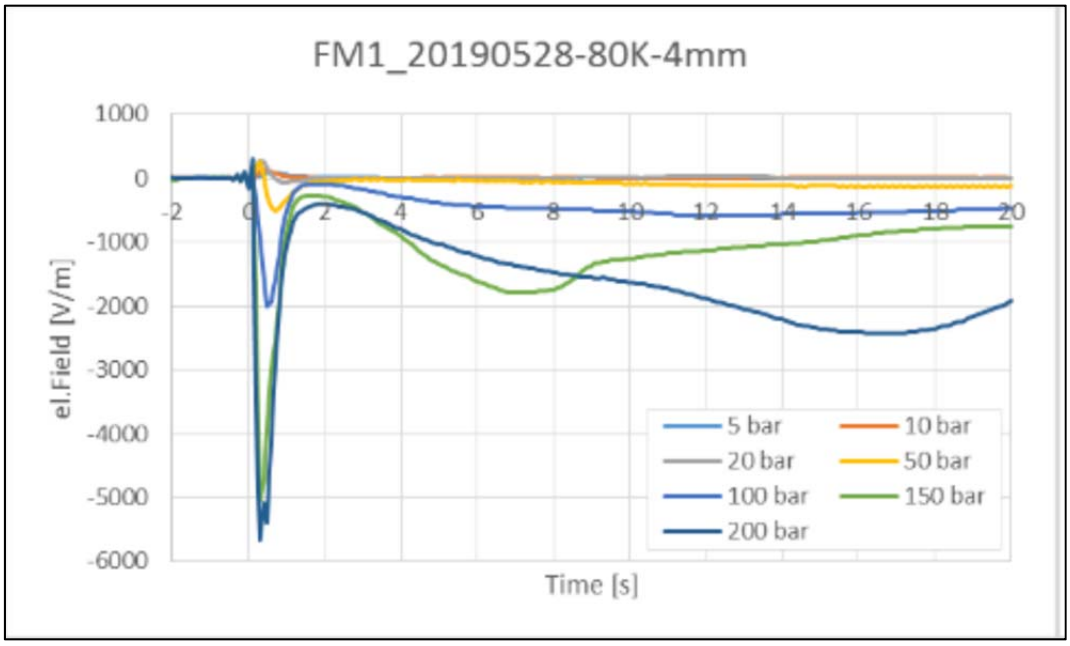

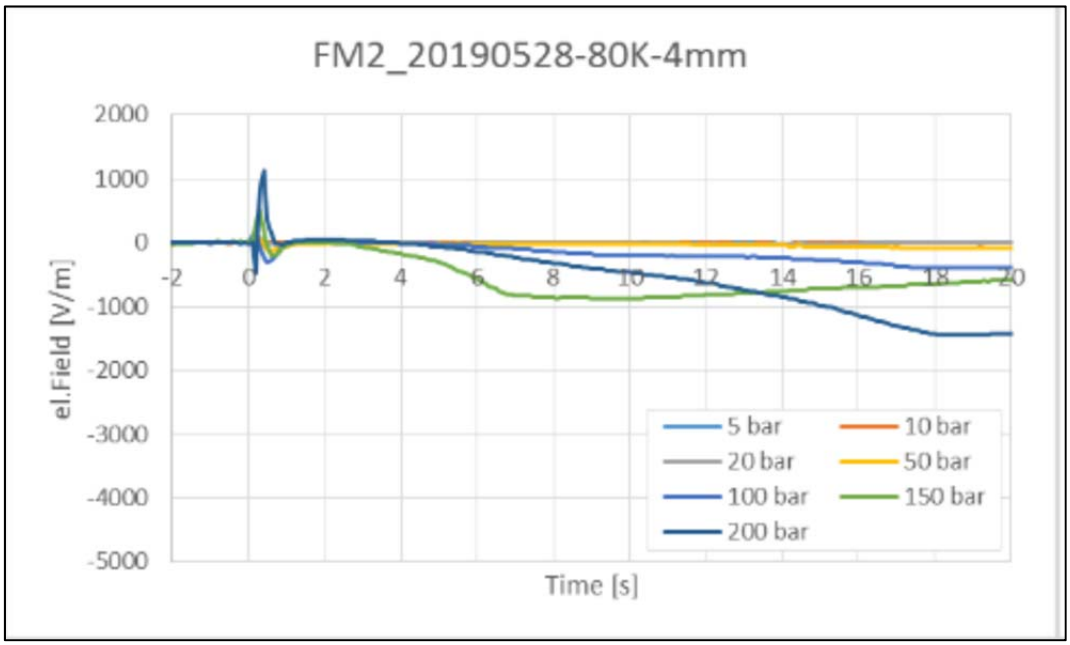

Figure 11: Electrostatic field measurements with field mill FM1 and FM2 for blow-down of up to 200 bar hydrogen at standard nitrogen boiling temperature (Friedrich, Veser, & Jordan, 2020)

Figure 12 shows the maximum and minimum electrostatic field strength measured at the field mills for pressures from 5 to 200 bar with a starting temperature of 80 K in the pressure reservoir. The figure again demonstrates that the direction of the field measured by the field mills might be opposite, and that the intensity of the signal is stronger in the record of field mill closest to the release nozzle.

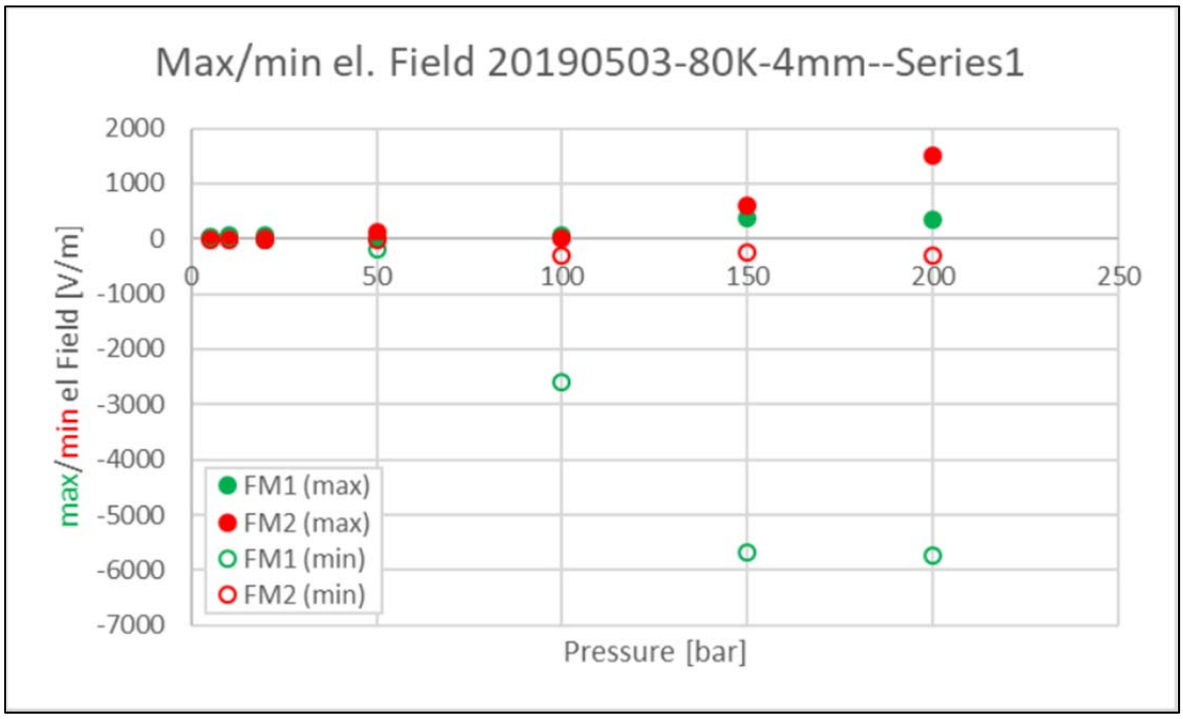

Figure 12: Maximum and minimum electrostatic field strength measured at field mill FM1 and FM2 for pressures from 5 to 200 bar with a starting temperature of 80 K in the pressure reservoir (Friedrich, Veser, & Jordan, 2020)

These tests showed high electrostatic fields generated, especially for high initial pressure levels. Supported by data from some precursor tests, it is assumed that the generation of the electrostatic field is associated with ice crystals formed on the release nozzle before the actual release; breaking off of these ice crystals and subsequent entrainment during the initial phase of the gas discharge lead to field generation.

Despite the relatively high electrostatic fields observed in the experiments no spontaneous ignition of the released jet was observed. However, such strong electric fields for high pressure releases, pressures considerably higher than those associated with liquid hydrogen tanker deliveries, may suggest a greater electrostatic ignition risk is present than with lower pressure releases.

4.2.2. Moderate pressure, up to 5 bar, and low temperature, down to 30 K, experiments (Friedrich, Veser, & Jordan, 2020)

The second facilities utilised liquid hydrogen and allowed experiments to be performed at temperatures down to 30 K but was limited to a pressure of 5 bar. Despite the low initial pressures used, considerable electric fields were measured.

As detailed above, cold jets at 30 K were again found to generate relatively strong electrostatic fields, but no test showed a spontaneous ignition. As for Section 4.2.1, the observed charging seems to be generated by ice crystals breaking off the nozzle and entering the hydrogen flow, these ice crystals were seen to form on the release nozzle before the tests.

During these experiments it was found that strong changes in the field strength were observed during the first tens of seconds. The field values were considerably higher during the release of liquid hydrogen at 30 K, than for gaseous hydrogen release at 80 K, discussed in Section 4.2.1, but in contrast the field values seem to decrease with increasing initial pressure level; this is shown in Figure 13.

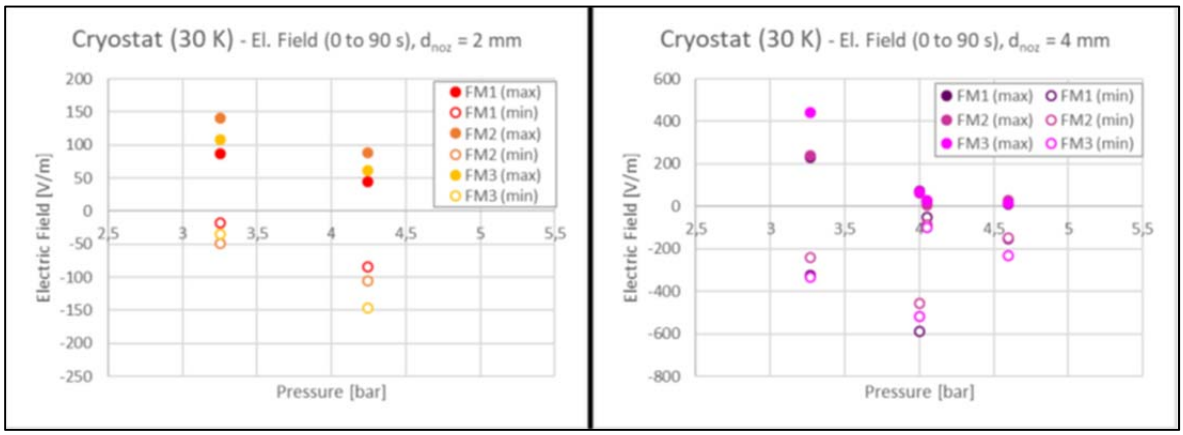

Figure 13: Maximum and minimum electrostatic field strength measured at the three field mills during the first 90 s of the liquid hydrogen-releases (Friedrich, Veser, & Jordan, 2020)

In some cases, especially for liquid hydrogen releases, strong fluctuations of the field values were also observed much later in the release. These fluctuations may have been caused by environmental influences outside the control of the experimental team (eg wind direction and strength) but could also have been caused by finger-like structures that formed at the tip of the nozzle during the release as shown in Figure 14. These structures were most likely formed of solidified air components and were blown away from time to

time by the plume or just fell due to their weight. However, a correlation between the removal of the structures and strong field fluctuations has not yet been fully evaluated,

Figure 14: Photo of the "finger-like" structures that formed at the tip of the nozzle during this experiment (Friedrich, Veser, & Jordan, 2020)

The fields measured in these tests at 5 bar, were considerably higher than those measured in the tests discussed in section 4.2.1, but in contrast the field values seem to decrease with increasing initial pressure level, it is important to note that the pressure range investigated here is much smaller than the range investigated in section 4.2.1.

5. Conclusions

Below are listed the main highlights and results from the experimental campaigns.

For all environmental conditions investigated, the resulting hydrogen flame was invisible to the naked eye and the ignition process was effectively silent. As the ambient temperature was reduced to -120 C the lower flammable limit increased by 1% and the upper flammable limit decreases by 10%.

For a concentration of 20% hydrogen in air, at atmospheric temperature and pressure the minimum ignition energy was found to be of 18 μJ; at -100°C the minimum ignition energy was found to be 50 μJ. The minimum ignition energies increase as the temperature decreases.

The critical hot surface ignition temperature of hydrogen-air mixtures is close to 600°C, which is very close to the autoignition temperature.

When various ground surface substrates were investigated gravel demonstrated some unique behaviour when compared to the other substrates investigated. It is porous to the liquid hydrogen and therefore able to hold higher liquid hydrogen amounts at stable temperatures; for some time after the initial spill this can condense out air components that accumulate in the free space in between the substrate particles. After ignition of any cloud above the pool, these condensed air components vaporize again and by this enforce the loads of the explosion observed.

After a liquid hydrogen release, where the liquid hydrogen was in excess, solid accumulation of air occurred. This mass of solid air was shown to incorporate liquid hydrogen plus other condensed components of air. Ignition trials indicated that the solid samples could support a flame but did not exhibit rapid or explosive burning.

Ground level jet releases of liquid hydrogen in a wide range of circumstances may allow the accumulation of condensed air; the composition of this condensate has the potential to support combustion and is thought to encourage a deflagration to detonation transition in the event of the vapour phase, above the condensed air and hydrogen mixture, undergoing combustion. This may have to be considered as part of a risk assessment process for such events alongside jet fire and vapour cloud explosions.

More experimental and modelling work to investigate the mixing and deposition of solid air during contact with cryogenic hydrogen is required. It would be particularly important to know how the risk changes with the scale of release.

It was found for both water spray and water jet that contact between water and liquid hydrogen will not necessarily cause a rapid phase transition, but this does not rule out such energetic events occurring under other circumstances. Emergency water spray suppression through sprinklers and monitors (water jets) may be used to control the flow or accumulation of liquid hydrogen without a high risk that a rapid phase transition may occur.

Where the liquid hydrogen forms a jet upon release, a transient electrical field can be measured, but a charged plume forming from an established cryogenic jet is unlikely.

The flow of liquid hydrogen in pipes can cause electrostatic charge to accumulate and certain conditions encourage this. The charging does not form inside the hydrogen flow, but on the substances or objects that the hydrogen interacts with. When charge accumulation is recorded this is always part of the two-phase flow section of the

experiment. It is therefore essential for safe working that either the liquid hydrogen pipework is designed so that the development of two-phase flow is limited, through vacuum insulation for instance, or the pipework contains no electrically isolated sections. For a fixed facility, maintaining continuity to earth and paying attention to objects in the potential path of a release, would limit the likelihood of electrostatic charging and therefore limit the hazard.

Strong electrostatic fields, around 6000 Vm^{-1}, were found for cold gaseous jets, 80 K, releases of hydrogen, especially where high initial pressure levels were utilised. These field strengths were determined to show values typically 100 times larger than the fields measured for corresponding releases at ambient temperature, but no spontaneous ignition events occurred. The observed static electricity seems to be generated by ice crystal formation on the release nozzle before and during the tests and break off of these ice crystals and entrainment into the gas discharge during the initial release.

When cold jets of liquid hydrogen (30 K) were released they were found to generate strong electrostatic fields, again because of ice crystals being entrained into the jet, again no spontaneous ignition events occurred. Strong changes in the field strength were observed during the first tens of seconds. The field values were considerably higher during the release of liquid hydrogen, at 30 K, than for gaseous hydrogen, at 80 K.

The potential for electrostatic ignition as a result of accidental releases at up to 5 bar appears low providing the gas assets are earthed.

6. References

Atkinson, G. (2020). Experiments and analyses of condensed phases, PRESLHY deliverable D4.8.

British Standards Institution. (2013). PD IEC/TS 60079-32-1:2013 Explosive atmospheres. Electrostatic hazards, guidance. London: British Standards Institution.

Cassutt, L., Biron, D., & Vonnegut, B. (1961). Electrostatic hazards associated with the transfer and storage of liquid hydrogen. Advances in Cryogenic Engineering: Proceedings of the 1961 Cryogenic Engineering Conference, (pp. 327-335). University of Michigan Ann Arbor.

Friedrich, A., Veser, A., & Jordan, T. (2020). Summary of experiment series E4.2 (Electrostatic) results, PRESLHY deliverable D4.5.

Friedrich, A., Veser, A., Gerstner, J., Kuznetsov, M., & Jordan, T. (2021). Summary of experiment series E4.4 (POOL-Facility) results, PRESLHY deliverable D4.7.

Hall, J. (2014). Ignited releases of liquid hydrogen. Buxton: Health and Safety Executive.

Hooker, P., Royle, M., Gummer, J., Willoughby, D., & Udensi, J. (2011). Self Ignition of Hydrogen by various mechanisms. Symposium series No. 156 Hazards XXII. Health and Safety Laboratory.

Lyons, K., & Hooker, P. (2020). Summary of experiment series E4.3 (Electrostatic Ignition) results, PRESLHY deliverable D4.6.

Lyons, K., Coldrick, S., & Atkinson, G. (2020). Summary of experiment series E3.5 (Rainout) results, PRESLHY deliverable D3.6.

Lyons, K., Proust, C., Cirrone, D., Hooker, P., Kuznetsov, M., & Coldrick, S. (2020). Theory and analysis of ignition with specific conditions related to cryogenic hydrogen, PRESLHY deliverable D4.1.

Proust, C. (2021). Summary of experiment series E4.1 results (Ignition parameters), PRESLHY deliverable D4.4.

Royle, M., & Willoughby, D. (2014). Releases of unignited liquid hydrogen. Buxton: Health and Safety Executive.